ACCURACY OF DIESEL ENGINE COMBUSTION METRICS OVER THE FULL RANGE OF ENGINE OPERATING CONDITIONS

Peter G. Dowell, Sam Akehurst, Richard D. Burke

Dept. of Mechanical Engineering, University of Bath, Bath, UK, email: R.D.Burke@bath.ac.uk

Key Words: Combustion Analysis, Diesel, Rate of Heat Release, Experimental diagnosis, Measurement Errors

ABSTRACT

Measuring and analyzing combustion is a critical part of the development of high efficiency and low emitting engines. Faced with changes in legislation such as Real Driving Emissions and the fundamental change in the role of the combustion engine with the introduction of hybrid-electric powertrains, it is essential that combustion analysis can be conducted accurately across the full range of operating conditions. In this work, the sensitivity of five key combustion metrics is investigated with respect to eight necessary assumptions used for single zone Diesel Combustion analysis. The sensitivity was evaluated over the complete operating range of the engine using a combination of experimental and modelling techniques. This provides a holistic understanding of combustion measurement accuracy.

For several metrics, it was found that the sensitivity at the mid speed/load condition was not representative of sensitivity across the full operating range, in particular at low speeds and loads. Peak heat release rate and indicated mean effective pressure were found to be most sensitive to the determination of top dead center (TDC) and the assumption of in-cylinder gas properties. An error of 0.5° in the location of TDC would cause on average a 4.2% error in peak heat release rate. The ratio of specific heats had a strong impact on peak heat release with an error of 8% for using the assumption of a constant value.

A novel method for determining TDC was proposed which combined a filling and emptying simulation with measured data obtained experimentally from an advanced engine test rig with external boosting system. This approach improved the robustness of the prediction of TDC which will allow engineers to measure accurate combustion data in operating conditions representative of in-service applications.

NOMENCLATURE

1.1 Symbols

a_{1-4}	Model fitted parameters	
AFR_{stoich}	Stoichiometric air fuel ratio	
C_{arr}	Arrhenius model constant (Fitted)	
C_{CO_2}	Volumetric concentration of CO2	%
C_d	Orifice Discharger coefficient	
C_{evap}	Fuel Evaporation model constant	
C_{mag}	Magnussen model constant (Fitted)	
C_{mod}	Chemla diffusion Combustion model constant (fitted)	J/kg ºCA
c_p	Specific heat capacity at constant pressure	J/kgK
c_V	Specific heat capacity at constant volume	J/kgK
d_{noz}	Injector Nozzle diameter	m
H	Enthalpy	J
HR_{max}	Peak rate of heat release	
h	Specific enthalpy	J/kg
$IMEP$	Indicated mean effective pressure	Pa
k	Turbulence density	m^2/s^2
K_{dw}	Dry/wet correction factor for CO2 emissions measurement	
LCV	Lower Calorific Value of fuel	J/kg
m	mass	Kg
N_{eng}	Engine Speed	Rev/min
n	Polytropic exponent for 2- and 3- point pressure referencing methods	
n_0	Assumed polytropic exponent for 3-point pressure referencing method	
n_{cy}	Number of cylinders	
p	pressure	Pa
Q_C	Net Heat energy from combustion	J
Q_{HT}	Heat transfer through cylinder walls	J

R	Gas constant	J/kgK
R^2	Coefficient of Determination	
T	Temperature	K
T_a	Fuel Activation Temperature	K
t	time	s
U	Internal energy	J
u_{CO2}	Relative density constant for CO2 emissions measurement	
V	Volume	m^3
W	Work	J
x	Proportion of fuel	
Y	Mass fraction	
$\boldsymbol{\alpha_{TDC}}$	Angle of mechanical top dead centre	^{o}
γ	Ratio of specific heats	
η_{vol}	Volumetric Efficiency	
θ	Crank Angle	^{o}
λ	Stoichiometric ratio for premixed combustion	
ρ	density	Kg/m^3
τ	Delay time constant	s^{-1}
χ_{EGR}	Fraction of EGR by mass	
Ψ	Blow-by flow passage flow coefficient	

1.2 Subscripts

air	Fresh air
$avail$	Available fuel
BDC	Bottom Dead Centre
b	Burnt gases
bb	Blow By flow
CO_2	Carbon Dioxide
cc	Crank Case
ch	Chemical Ignition delay

cy	In-cylinder
$diff$	Diffusive combustion
EGR	Exhaust gas recirculation
eoc	End of Combustion
exh	Flow through exhaust valves
f	fuel
ID	Ignition Delay
in	Inlet manifold
inj	Injected
inl	Flow through intake valves
$liqu$	Liquid
$main$	Main injection or combustion event
max	Peak/maximum
$meas$	Measured
ph	Physical ignition delay
pre	Pre-mixed combustion
$resid$	Residuals
soc	Start of combustion
SOI	Start of Injection
vap	evaporated

1.3 Abbreviations

ATDC	After top dead centre
BMEP	Brake Mean Effective Pressure
CA	Crank Angle
CO_2	Carbon dioxide
EGR	Exhaust Gas Recirculation
EOI	End of Injection
F&E	Filling and Emptying (model)
HiL	Hardware in the Loop

IVC	Inlet Valve Closing
IMEP	Indicated Mean Effective pressure
MCC	Mixing Controlled Combustion
NO_x	Oxides of nitrogen
RoHR	Rate of Heat Release
SOC	Start of Combustion
SOI	Start of Injection
SSE	Sum Squared Error
TDC	Top dead centre

1 INTRODUCTION

The processing of measured in-cylinder pressure via a single zone model to provide estimates of Indicated mean effective pressure (IMEP) and combustion Rate of Heat release (RoHR) is a vital tool for the analysis, development, and design of engines [1, 2]. Real time combustion analysis for lab and control strategies make use of this simple combustion analysis technique because of its computing efficiency. Parameters derived from the RoHR such as start of combustion (SOC), burn rates, peak temperatures and the combustion mode (diffuse or pre-mixed) can reveal important trends in the engine's performance and these metrics are also useful for novel control applications for advanced combustion modes, emissions and noise [1]. The combustion metrics are also vital for the parameterization of predictive engine models to link the engine's operating condition (speed, load, boost pressure, etc.) to its behavior (burn rate, efficiency, thermodynamic and heat transfer losses) [3-5]. It is therefore crucial to have an accurate and precise estimate of heat release from measured in-cylinder pressure.

The computation of combustion metrics from measured in-cylinder pressure involves many assumptions, each contributing to overall uncertainty. The aim of this work is to assess the uncertainty of the key combustion metrics against these assumptions, across the complete operating range of the engine. This is essential as combustion research must now analyse and improve performance across a broad range of operating conditions in response to changes is legislation such as Real Driving Emissions (RDE).

After presenting a review of previous works and experimental configuration, the results will be split into two parts. Firstly, experiments from a 2.0L Diesel engine will be used to evaluate overall sensitivity to eight parameters in the pressure data analysis. Secondly, for these eight factors, the sensitivity of different assumptions will be compared.

2 BACKGROUND

Five key combustion parameters have typically been assessed in the literature for combustion analysis: the indicated mean effective pressure (IMEP), the peak net rate of heat release (HR_{max}), the total net heat release from combustion (Q_c), the start of combustion (SOC) and the total heat loss through the cylinder walls (Q_{HT}). Combustion temperature can also be considered as a key combustion metric, however it's calculation does not involve any additional assumptions than those used for these metrics. These quantities can be calculated based on a measured in-cylinder pressure: IMEP is calculated from indicated work (equation 1).

$$dW = p_{cy} dV_{cy} \quad (1)$$

Heat release parameters are calculated by applying the first law of thermodynamics to the combustion chamber such that the rate of heat release from combustion is the sum of the change in internal energy, heat and work transfers and enthalpy transfers through the valves and blow-by gases (equation 2).

$$dQ_c = dU - dQ_{HT} - dW + dH_{inl} - dH_{exh} - dH_{bb} \quad (2)$$

For Diesel Engines combustion occurs with the intake and exhaust valves closed. The change in internal energy can be calculated from equation 3 where the in-cylinder temperature is calculated using the measured pressure and the perfect gas law (equation 4).

$$dU = m_{cy} c_{p,cy} dT_{cy} \quad (3)$$

$$T_{cy} = \frac{p_{cy} V_{cy}}{m_{cy} R} \quad (4)$$

Equations 1-4 show that to perform these calculations the following assumptions are required:

1. An estimate of cylinder volume (V_{cy}), in phase with the pressure measurement
2. A reference pressure to determine the absolute value of in-cylinder pressure
3. An accurate calibration of the pressure transducer
4. A low pass filter to remove measurement noise from the pressure measurement
5. An estimate of the mass of gas trapped in the combustion chamber (m_{cy})
6. An estimate of the compression ratio of the engine (used in the calculation of V_{cy})

7. An estimate of the convective heat transfer between the combustion gases and the cylinder walls (Q_{HT})
8. The estimate of blow-by mass flow escaping the cylinder between the piston rings and the cylinder wall (to determine H_{bb})

Table 1 summarizes the sensitivity of the five combustion metrics to the seven parameters based on three studies of a simulated engine [5], a motored engine [6] and a fired engine [7]. Table 1shows that IMEP and peak RoHR are very sensitive to the correct determination of TDC position: this is the correct phasing of pressure measurement and volume calculation. In one study, it is shown that under fired condition, a 0.5°CA error in pressure phasing resulted in a 3.6% error in IMEP. This has led some authors to recommend a tolerance of ±0.1 CA for TDC position [6-8].

Table 1 also suggests that, under fired conditions, reference pressure and compression ratio have little influence over peak heat release (HR_{max}), but have a significant effect on start of combustion (SOC). The greater influence on HR_{max} under motored condition is likely to come from the sensitivity to heat transfer, which makes up all the heat release in this case.

Transducer calibration error is proportional to IMEP and has a significant effect on HR_{max}. This is more significant than reference pressure because an error in reference pressure is only significant at low pressures. An error in transducer calibration can result in a proportional error at all pressure magnitudes. Thermal shock can cause unrealistically low pressure during the expansion and exhaust blowdown stroke [6, 9] due to the high temperatures occurring during combustion causing changes in the mechanical properties of the quartz crystal, and distortion of the diaphragm of the piezoelectric pressure sensor [9]. As speed increases, the effect of thermal shock reduces since the flame impinges on the diaphragm for a shorter time [9]. It can result in errors in pressure up to 1 bar, and has a knock-on effect on the calculation of IMEP, resulting in errors between -9% and +2% [6].

Several correlations exist for correcting for thermal shock [9, 10]; however, these rely upon constants derived experimentally using a reference sensor which may not be readily available. Ultimately, the most robust way of reducing thermal shock is the use of a water-cooled pressure sensor [6, 9, 10].

Cylinder mass has a small effect on most RoHR parameters, but is most significant when calculating heat transfer which is due to its effect on cylinder temperature. Heat transfer is shown to have a large effect on HR_{max} and SOC during fired conditions.

2 METHODOLOGY

The parameters affecting the accuracy of the combustion metrics were investigated over the complete operating range of a 2.0L Diesel engine. The results presented in this paper are derived from two sources:

1. Measurements from an engine dynamometer
2. Simulations from a correlated filling and emptying model.

2.1 Experimental Configuration

The engine was installed on a transient dynamometer facility and two data acquisition systems were used: a CP Engineering Cadet Automation System monitoring low frequency data at a rate of 20Hz and a D2T Osiris system capturing indication data for every 0.1°CA. A summary of key instrumentation is provided in Table 2.

A series of steady-state measurements were taken with a fully warm engine covering the full engine speed/load envelope (Figure 1). For each operating condition, data was recorded after a 5 minute settling time and averaged over 30 seconds (low frequency data) or 100 cycles (indicated data).

Additional motored engine test points were measured at different engine speeds with no fueling. For these tests the air path was replaced with a boosting emulation system illustrated in Figure 2. This configuration allows the engine to be motored whilst maintaining intake manifold boost pressure, meaning motored cycles with variable trapped mass can be observed.

2.2 Filling and emptying model

The filling and emptying model is used to predict the trapped mass in the cylinder for each cycle. Whilst the fresh air charge is easily measured on an experimental facility, or could be decided from inlet manifold conditions known volumetric efficiency, this cannot capture with any accuracy the trapped residuals. Therefore the filling and emptying model is implemented and verified and against the fresh air flow measurement.

The filling and emptying model considered only the high-pressure gas path between the outlet of the charge air cooler and the inlet to the turbocharger turbine. The model comprises four control volumes linked by the intake, exhaust and EGR valve (Figure 3). The model calculates the flow through each of the valves and heat transfer in the exhaust manifold and EGR cooler using empirical models. In each control volume, the gas is considered to be composed of up to three species: fresh air, fuel and burnt fuel and air. A gas properties model was used to determine the bulk fluid properties in each case.

Each of the volumes has a state of pressure, temperature and mass. The mass flow through the combustion chamber valves is calculated based on the known pressure ratio and area of the valve with equation 5.

$$\dot{m}_{valve} = A_{valve} C_d \frac{p_i}{\sqrt{RT_i}} \Psi\left(\frac{p_j}{p_i}, \gamma\right) \qquad (5)$$

Equation 5 uses an empirically derived discharge coefficient C_d and a flow function (Ψ) governed by the pressure ratio between the downstream pressure (subscript *j*) and the upstream stagnation pressure (subscript *i*) and related to the ratio of specific heats (γ) as described in equation 6.

Since the instantaneous flow velocities are relatively small, the static pressure upstream of the valves can be taken to be approximately equal to the stagnation pressure [11]. The reference valve area for inlet and exhaust valves depends on the valve lift and geometry as described in equation (7).

The model has been shown to predict air-flow through the engine with a coefficient of determination of 0.99 both with and without EGR flows [12].

$$\Psi = \begin{cases} \left(\frac{2}{\gamma+1}\right)^{\frac{1}{\gamma-1}} \sqrt{\frac{2\gamma}{\gamma+1}} & if\ 0 < \frac{p_2}{p_1} < \left(\frac{2}{\gamma+1}\right)^{\frac{1}{\gamma-1}}; \\ \sqrt{\left(\frac{2\gamma}{\gamma-1}\right)\left[\left(\frac{p_2}{p_1}\right)^{\frac{2}{\gamma}} - \left(\frac{p_2}{p_1}\right)^{\frac{\gamma+1}{\gamma}}\right]} & if\ \left(\frac{2}{\gamma+1}\right)^{\frac{1}{\gamma-1}} < \frac{p_2}{p_1} < 1; \end{cases} \quad \begin{cases} -\sqrt{\left(\frac{2\gamma}{\gamma-1}\right)\left[\left(\frac{p_1}{p_2}\right)^{\frac{2}{\gamma}} - \left(\frac{p_1}{p_2}\right)^{\frac{\gamma+1}{\gamma}}\right]} & if\ 1 < \frac{p_2}{p_1} < \left(\frac{2}{\gamma+1}\right)^{\frac{1}{\gamma-1}} \\ -\left(\frac{2}{\gamma+1}\right)^{\frac{1}{\gamma-1}} \sqrt{\frac{2\gamma}{\gamma+1}} & if\ \left(\frac{2}{\gamma+1}\right)^{\frac{1}{\gamma-1}} \leq \frac{p_2}{p_1} \end{cases}$$

$$A_{valve} = \begin{cases} \pi L_{valve} \cos\beta \left(D_{valve} - 2w_{seat} + \frac{L_{valve}}{2} \sin 2\beta\right) & if\ L_{Low} \geq L_{valve} > 0 \\ \pi (D_{seat} - w_{seat}) \sqrt{(L_{valve} - w_{valve} \tan\beta)^2 + w_{valve}^2} & if\ L_{High} > L_{valve} > L_{Low} \\ \frac{\pi}{4}\left(D_{port}^2 - D_{seat}^2\right) & if\ L_{valve} \geq L_{high} \end{cases}$$

2.3 Sensitivity analysis

Firstly, sensitivity was assessed by introducing perturbations to the different measured parameters in the rate of heat release calculation. The magnitude of the perturbations imposed on each factor are summarized in table 3 and were determined based on those seen in the literature (summarized in table 1). The resultant variation in each combustion metric was quantified across the full engine speed and load operating range. The sensitivity was quantified for the specific engine in this study as a fraction of the sensitivity at the mid load/mid speed point (2500rpm, 120Nm).

Secondly, the individual steps in the calculation were investigated in further detail, looking at how different assumptions and algorithms impact on the resultant combustion metric quantities. The details of these assumptions are described in the following sections.

2.3.1 Phasing of cylinder volume

The phasing of the cylinder volume is achieved by correctly identifying the position of smallest volume (top dead centre). This is typically determined using measured pressure from a motored engine cycle. Figure 4 illustrates the concept of the loss angle which is the difference between peak observed pressure (thermodynamic TDC) and the point of minimum volume (volumetric TDC) when the engine is motored. To correctly phase volume and pressure, this loss angle must be correctly estimated [13-19]. In this paper, three methods are compared for evaluating the loss angle:

Method no.1: The 'loss function' method [16]

This method is based on approximating the loss angle by considering the effects of heat transfer and blow-by mass by considering the thermodynamic process. The method uses the insensitivity of thermodynamic losses to the loss angle at the points of maximum and minimum relative volume change meaning the function can be evaluated with an unknown loss angle. Some simplifying assumptions with respect to heat transfer and blow-by are then used to determine the loss angle location.

Method no.2: The 'inflection point' method [20]:

This method is based on calculating the polytropic exponents for the compression and expansion processes of a motored cycle pressure trace. The exponents are evaluated as a function of volume and volume change at the pressure inflexions points, i.e. when the second derivative of pressure are zero. A loss angle is assumed and iterated until the two polytropic exponents satisfy an empirical criterion.

Method no. 3 the filling and emptying method

The filling and emptying method uses the model described in section 3.2 to estimate the loss angle under motored conditions. This simulated loss angle is then used to adjust the position of top dead centre for a measured motored cycle. The experimental motored cycle measurement is performed first. Then the simulated cycle is calculated by imposing boundary conditions measured during the motoring cycle (boundary conditions are pressure and temperature in the intake manifold and pressure in the exhaust manifold). The model will predict in-cylinder pressure and therefore also the angle of maximum cylinder pressure during the simulated motored cycle. This is then compared directly to the geometric TDC which is an input to the filling and emptying model. Finally the simulated loss angle is used as the offset between peak cylinder pressure in the measured motored cycle and actual geometric TDC. This approach is based on the assumption that the filling and emptying model will provide

an accurate estimate of cylinder pressure history. One critical point is the heat transfer model which in this work was determined from the work of Finol [21]. To compare the three approaches, the motored cycles were used. As an absolute measurement of the location of TDC was not possible in this work so the methods are compared based on their consistency across the engine operating space. An arbitrary value of loss angle was assumed of 0.6°CA at 1000rpm, 101kPa boost (see Figure 7) which was an average value for all methods. In this way, the methods are compared based on their ability to predict the change in loss angle for different engine speeds and trapped mass. The assumed location of TDC will subsequently be referred to as *Measured**.

2.3.2 Pressure referencing

Piezoelectric pressure sensors do not give an absolute value of pressure; therefore, the measured pressure signal needs to be 'pegged' to a known reference pressure. Three approaches will be compared by applying them to measured data from the full fired engine map (Figure 1). The prediction of absolute pressure was compared to that predicted by the filling and emptying model.

- Pegging to inlet manifold pressure at inlet manifold pressure at intake valve closing (IVC) [5, 7, 14, 22]. Assuming the cylinder is effectively stationary at this point, there is little change in volume and the inlet manifold pressure will equal in-cylinder pressure. This approach ignores wave dynamics in the manifold [14, 23].
- Fixed Polytropic approach where the reference pressure is calculated using two points (1 and 2) between intake valve closing and start of combustion and an assumed polytropic exponent n such that 1.25≤ n ≤1.38 [22] (see equation 8).

$$\Delta p = p_{cy}(\theta_1) - \frac{p_{cy}(\theta_2) - p_{cy}(\theta_1)}{\left[\frac{V_{cy}(\theta_1)}{V_{cy}(\theta_2)}\right]^n - 1} \qquad (6)$$

- A three-point method with a calculated polytropic exponent. The exponent is calculated using the Taylor expansion in equation 7 [23]. Although in principle more accurate, the three-point method is more sensitive to noise in the measured pressure signal.

$$n = n_0 + Z_1\left[\frac{p_{cy}(\theta_2) - p_{cy}(\theta_1)}{p_{cy}(\theta_3) - p_{cy}(\theta_1)} - Z_2\right] \qquad (7)$$

$$Where\ Z_1 = \frac{K^{n_0} - 1}{J^{n_0} \cdot \ln(J) - (Z_2 \cdot K^{n_0} \cdot \ln(K)}, \quad Z_2 = \frac{J^{n_0} - 1}{k^{n_0} - 1}, \quad J = \frac{V_{cy}(\theta_1)}{V_{cy}(\theta_2)}, \quad K = \frac{V_{cy}(\theta_1)}{V_{cy}(\theta_3)}$$

2.3.3 Pressure signal filtering

A nominal number of cycles need to be captured to characterize a steady state operating point: averaging can then be used to remove random noise but systematic noise must be removed by filtering [24]. Three smoothing techniques will be compared: a digital filtering [24, 25]; polynomial regression fitting [16, 26] and smoothing splines [27]. Although a very large number of digital filters can be used, on the case of combustion analysis these will all be low-pass filters. The comparison of these different filter types is beyond the scope of this work, and only a single filter is considered for comparison with the polynomial and smoothing spline techniques. The filter used in this work is a Butterworth filter, with cut-off frequency 314kHz and order 8. However, a double filtering approach is used (forward and reverse) to ensure no phase lag is introduced by the filtering[1]. This filtering approach effectively doubles the order of the filtering process.

2.3.4 Trapped mass estimate

Two methods for estimating the mass trapped in the cylinder will be compared: the *perfect gas law* method and the *delta-p* method [4, 28-30]. Trapped mass predicted from the F&E model was used to compare the estimation from the two methods.

The perfect gas law method uses the inlet manifold conditions and the volume at bottom dead center (BDC) to calculate trapped mass (equation 8). This method relies on an estimate of the volumetric efficiency and two assumptions will be compared: the first assuming 100% volumetric efficiency (labelled *perfect gas law method*) and the second using a mean volumetric efficiency determined from three operating points (labelled *corrected perfect gas law method*). The volumetric efficiency for this engine was determined based on measurements of fresh air flow into the cylinder; this was possible because there is no overlap between the intake and exhaust valves. Should this be the case, then the filling and emptying model is required for this estimation.

[1] The double filtering is achieved by using the Mathworks MATLAB "*filtfilt*" command.

$$m_{cy} = \overline{\eta_{vol}} \frac{p_{in} V_{cy,BDC}}{R T_{in}} \quad (8)$$

The *delta-p* method uses a mathematical regression of a pressure difference between 2 points in the compression phase of the cycle.

$$m_{cy} = a_1 \, \Delta p_{cy} - a_2 \quad (9)$$

$$Where\ a_1 = \frac{V_{cy}(\theta_1)\, V_{cy}(\theta_2)^{\gamma}}{R\, T_{cy}(\theta_1) \left(V_{cy}(\theta_1) - V_{cy}(\theta_2) \right)},$$

$$a_2 = m_{resid,\ cy} + m_{f,cy}$$

The parameters a_1 and a_2 are calibrated at different speeds using measured trapped mass. At each operating speed, three of the eight operating points shown in Figure 1 were used to calibrate the values of a_1 and a_2.

2.3.5 In-cylinder heat transfer

Heat transfer by radiation and convection from the combustion gases to the cylinder wall are typically calculated using Newton's law of cooling and a heat transfer coefficient. The heat transfer coefficient is typically estimated using an empirical correlation. Three correlations were compared in this study: Woschni [4]; Hohenburg [11]; and a bespoke correlation created by Finol for the engine used in this study [21]. Figure 5 compares the crank angle resolved heat transfer coefficients.

The heat transfer models were compared by calculating fuel burnt from in-cylinder pressure data (using equation 10) and comparing this to fuel consumption from a gravimetric beaker. Any errors in the heat transfer model would directly impact on the calculated heat release from combustion.

$$m_f = \frac{1}{LCV_f} \int_{soc}^{eoc} \frac{dQ_c}{d\theta} d\theta \quad (10)$$

2.3.6 Gas composition and ratio of specific heats

The gas is split into three component species: air (a); burnt gas products (b); and fuel (f). The evolution mass fraction from inlet valve closing is estimated using the rate of heat release and fuel injection rate. The mixture properties were calculated by mass weighted average [5, 31].

Three assumption were compared for calculating the ratio of specific heats:

- A constant value based on average temperature [4]

- A temperature dependent model [32]
- A temperature and gas composition dependent model [31]

2.3.7 Blow-by

Blow-by enthalpy loss peaks around TDC where peak temperature and pressure occur simultaneously with combustion. Blow-by also has a secondary effect of increasing heat lost to the walls, since the drop in mass increases gas temperatures. Blow-by can be modelled as an isentropic discharge through a nozzle connecting the cylinder with the crankcase (see equation (5))[31]. For this work, the flow coefficient for blow-by Ψ was assumed a constant value of $\Psi = 0.532$ which produced very similar results when compared to the more complex model that includes chocking effects [5, 33]. A blow-by flow meter was used to measure the flow rate of gas from the crankcase back into the inlet manifold during the boosted motoring tests. This enabled measurement of blow-by mass at different speeds and gas loads for comparison against the two models using the following equations:

$$\dot{m}_{bb} = A_{bb} C_{d,bb} \frac{p_{cc}}{\sqrt{R T_{cc}}} \psi\left(\frac{p_{cy}}{p_{cc}}, \gamma\right) \quad (11)$$

$$m_{bb} = \int \dot{m}_{bb} dt \quad (12)$$

$$m_{bb,meas} = \frac{\rho_{cc} \dot{V}_{bb,meas}}{2 N_{eng}\, n_{cy}} \quad (13)$$

3 RESULTS AND DISCUSSION

Figure 6 and Table 3 show the sensitivity of the five combustion metrics to seven parameters used in the processing of combustion pressure data. The contours in Figure 6 are normalised to the point of highest sensitivity. The results in Table 3 tabulate the sensitivity at the mid-point of the operating map (2500rpm, 120Nm) and allow for direct comparison to the results from table 1.

The parameters which have the most influence over the combustion metrics are TDC position and ratio of specific heats. Both inputs affect the shape of the RoHR. IMEP is mainly sensitive to changes in TDC position and transducer calibration. HR_{max} is affected by most parameters whilst SOC is most sensitive to TDC position. Total heat loss through the cylinder wall (Q_{HT}) is sensitive to most parameters, though it is important to note that any changes in Q_{HT} will only contribute a small amount to gross heat release. Compression ratio was found to have little impact on any of the output parameters tested.

Figure 6 shows that most combustion metrics are more sensitive at lower engine speeds and torques. Therefore, extra caution should be exercised in working or calibrating models in this area since the errors can rise to double their mean value. The following sections will provide more details on the effects of the individual factors.

3.1 Top dead center position

Figure 6 shows that most of the sensitivity of IMEP, total heat release and start of combustion are primarily load dependent. This is because the phasing of pressure and volume affects the calculation of work during compression and expansion, which is more significant at low loads. Maximum RoHR and heat transfer have a speed and load dependence, with maximum RoHR being more sensitive at higher speeds/loads and the opposite being true for heat transfer.

Table 4 shows that the filling and emptying method matches the trend in measured α_{TDC} the best, with highest R^2 and smallest maximum error. All three methods have a mean error within 0.1°CA; however, only the filling & emptying method has a maximum error which is within this tolerance. It would be expected that the accuracy of this method will depend on the quality of the filling and emptying model.

Figure 7 shows that all three methods predict the trend in loss angle as engine speed and inlet manifold pressure increase. Qualitatively, the inflection point method predicts the shape of the trend the best; however, the change in TDC position over the range of speeds and inlet manifold pressures is over-predicted.

3.2 Pressure referencing

The results in Table 3 broadly agree with those found in table 1: they show that Q_c is most influenced by reference pressure. Figure 6 shows that Q_c errors decrease with torque, which is due to reference pressure counting for a smaller proportion of combustion pressures at high load.

Figure 8 shows that the fixed polytropic method and inlet manifold pressure method perform well, giving little error for all test points; whereas the variable polytropic exponent method yields consistently higher error, especially at high speeds.

Table 5 shows that the fixed polytropic method and the intake manifold method both perform broadly the same, however, the fixed polytropic constant method does result in less error and requires less instrumentation, so would be the preferred method. The variable polytropic constant method performs markedly worse.

3.3 Transducer calibration and pressure signal processing

Table 3 shows that there was a proportional response in IMEP, HR_{max} and Q_c for a variation in transducer calibration. There was almost no change in output sensitivity across the test points tested, as shown in Figure 6, with the exception of heat transfer which was more sensitive at low loads.

Figure 9 (a) shows the evolution of the maximum standard deviation of cylinder pressure as the number of cycles is increased. The maximum standard deviation is obtained by first evaluating the standard deviation of cylinder pressure at each crank angle for the number of cycles in consideration. The maximum observed standard deviation is then retained to give an indication of cycle-to-cycle variability. The results show that an average of over 50 cycles will be representative of the operating point Figure 9 (b) shows that when compared to the magnitude of the mean signal, the deviation is small and is mainly due to acoustic noise from combustion, indicating that it is most sensitive to load.

Figure 10 shows a comparison between the different filtering techniques. The low-pass Butterworth double filter (details provided in section 3.3) retains the shape of the pre-mixed pilot spike, but introduces oscillations between combustion events. The polynomial and spline fitting methods give similar results, but reduce the peak of the pilot spike. By applying a double spline technique with different degrees of filtering before and after SOC, this peak is captured yielding an acceptable result after the initial combustion event [27].

3.4 Trapped mass estimate

Table 3 shows that peak heat release and heat losses are most affected by the change in trapped mass and this agrees with table 1. In-cylinder mass determines the calculated temperature which directly affects Q_{HT} and the gas properties. The effect is reduced at higher load points as temperatures are dominated by combustion rather than work done on the gas (Figure 6).

Figure 11 and Table 6 show that the delta-p method has lower mean error than the perfect gas law method, but the perfect gas law method correlates better with the F&E data (evidenced by lower R^2 value, smaller maximum error and smaller standard deviation of error). This is due to the spread of error being greater when adopting the delta-p method, as a linear fit is being applied to a non-linear function. The perfect gas law method has a larger static error, but once this is 'corrected' by applying a volumetric efficiency measured at three operating points, the error is comparable to that produced by the delta-p method.

3.5 Compression ratio estimate

The results from Table 3 show that compression ratio has the most influence over Q_{HT} and SOC, with some effect on Q_c. This is similar to the effect of trapped mass, since compression ratio changes volume, which also directly affects the gas temperature calculation. Q_{HT} was found to be most sensitive to compression ratio at low loads. There was no definite trend for sensitivity of HR_{max} and SOC. Together with the low magnitude of error associated with changes in compression ratio, this suggests that the variation of this parameter (due to chamber deformation and cylinder-to-cylinder variance [5]) will not have a significant impact on the calculation of RoHR.

3.6 Heat transfer coefficient

Logically, Table 3 shows that Q_{HT} was proportional to the heat transfer coefficient. The heat transfer coefficient also affects SOC at low loads and peak heat release at high loads, suggesting that heat transfer distorts the RoHR signal.

Figure 12 shows that average error in total fuel burnt prediction (equation 10) is lower using Woschni's heat transfer model, with an error of ±5%, whereas the Finol and Hohenburg models larger errors of -6% to +10%. However, the Woschni model does have several disadvantages because it requires more calibration data (motored pressure and SOC data) and it produces discontinuities which can distort the gross heat release signal (see Figure 5).

3.7 Gas properties

The results in Table 3 show that HR_{max} , Q_c , SOC and Q_{HT} are all sensitive to the ratio of specific heats (γ). Because both SOC and HR_{max} are affected, the shape of RoHR is altered. From Figure 6, most of the combustion metrics are more sensitive to γ at low speed and load except for net heat released which is more sensitive at high loads.

Figure 13(a) shows the gas composition after SOC at the mid-load point in the engine map. A significant amount of air is converted into burnt gas during combustion. Fuel fraction barely exceeds 1% at most loads, so is less important compared to the burnt mass fraction. Figure 13(b) shows the influence that the different gas property models have on the ratio of specific heats and Figure 13(c) shows the effect this has on the RoHR.

In Figure 13(b), using an average value of gas properties underestimates gamma for most of the compression stroke, and overestimates it for the remainder of the cycle. Using a temperature based model gives a varying prediction of gamma, although after the main SOC it is overestimated compared to the component gas model.

From Figure 13(c), using an average value of gas properties can lead to a lower peak RoHR by up to 8% compared to the case where gamma is a function of both temperature and gas composition; the temperature based model is 3% lower. The effect of gas properties is more significant at high loads where the proportion of burnt gas is significant [31, 34, 35].

3.8 Blow-by mass

The literature suggested that blow-by mass has only a small influence on the in-cylinder parameters. Figure 14 shows the percentage contribution of blow-by losses to the total heat released over the engine speed torque map. It can be seen this is always less than 1.4% and generally more significant a low engine speeds and low engine loads.

4 CONCLUSIONS

The sensitivity of five combustion metrics was evaluated with respect to eight parameters. The analysis was performed across the complete speed/load operating region of a 2.0L Diesel engine. It was found that:

1. For several parameter/metric combinations, the sensitivity at the mid-operating point was not representative of the general trend across operating points. It is very important to understand this as future engine development must address the emissions requirements of Real Driving Emissions legislation. Most output parameters are more sensitive to changes in inputs at low speed / load points, which is representative of most city driving where combustion and emission control is most important.
2. The accuracy of top dead center had the largest effects on the accuracy of peak heat release rate (4.2% and 9.1% respectively). A new method for obtaining TDC position was proposed combining results form a filling and emptying model and motored engine test with external boosting. This method provides a high precision calibration of TDC which can increase combustion metric accuracy over the complete operating range of engine speeds and mass flows compared to other methods.
3. The accuracy of the ratio of specific heats (γ) also had a strong influence on the accuracy of heat release, mainly close to peak heat release rate where the temperatures are greatest. There is around 8% difference in peak heat release rate by assuming a constant value for γ compared to a temperature and composition dependent value. The effect of temperature is slightly greater than that of composition.

The findings from this work allows engineers to make an assessment of their combustion analysis tools and to make decisions on the parameters and algorithms to improve the accuracy of these measurements. This will allow greater confidence in assessing engine combustion performance over on-road representative duty cycles.

5 ACKNOWLEDGMENTS

The authors acknowledge the Engineering and Physical Sciences Research Council (EPSRC) funding under projects EP/C540883/1 and EP/C540891/1 and the Ford Motor Company for the supply of test hardware and data.

6 REFERENCES

[1] Lujan JM, Bermudez V, Guardiola C, Abbad A, *A methodology for combustion detection in diesel engines through in-cylinder pressure derivative signal*, Mechanical Systems and Signal Processing. 24(7): p. 2261-2275, 2010

[2] Brunt MFJ, Platts KC. Calculation of Heat Release in Direct Injection Diesel Engines, SAE Paper Number 1999-01-0187. 1999.

[3] Gatowski JA, Balles EN, Chun FE, Nelson FE, Ekchian JA, Heywood JB, *Heat Release Analysis of Engine Pressure Data*, SAE Paper Number 841359, 1984.

[4] Heywood, J.B., *Internal Combustion Engine Fundamentals*, 1988, New York: McGraw-Hill, ISBN: 0-07-100499-8

[5] Payri F, Molina S, Martin J, Armas O. Influence of measurement errors and estimated parameters on combustion diagnosis, Appl Therm Eng. 2006;26(2-3):226-36.

[6] Kuratle RH, Marki B. Influencing parameters and error sources during indication on internal combustion engines, SAE paper number 920233, 1992.

[7] Lapuerta M, Armas O, Bermudez V., Sensitivity of diesel engine thermodynamic cycle calculation to measurement errors and estimated parameters. Appl Therm Eng, 2000. 20(9): p. 843-861

[8] Lancaster DR, Krieger RB, Lienesch JH. *Measurement and Analysis of Engine Pressure Data,* SAE International; 1975, SAE Paper 750026

[9] Lee S, Bae C, Prucka R, Fernandes G, Filipi Z, Assanis DN., *Quantification of Thermal Shock in a Piezoelectric Pressure Transducer*, SAE International; 2005, SAE Paper 2005-01-2092

[10] Rai HS, Brunt MFJ, Loader CP., Quantification and Reduction of IMEP Errors Resulting from Pressure Transducer Thermal Shock in an S.I. Engine, SAE International; 1999, SAE Paper Number 1999-01-1329

[11] Hohenberg GF., *Advanced Approaches for Heat Transfer Calculations,* SAE International; 1979, SAE Paper Number 790825

[12] Dowell, P.D., *Real time heat release model of a HSDI Diesel engine*, PhD Thesis, 2012, Dept. of Mechanical Engineering, University of Bath, Bath

[13] Pipitone E, Beccari A, Beccari S., Reliable TDC Position Determination: a Comparison of Different Thermodynamic Methods Through Experimental Data and Simulations, SAE paper number 2008-36-0059

[14] Davis RS, Patterson GJ, *Cylinder Pressure Data Quality Checks and Procedures to Maximize Data Accuracy,* SAE International; 2006., SAE Paper Number 2006-01-1346

[15] Zeng, P. and Assanis, D., *Cylinder Pressure Reconstruction and its Application to Heat Transfer Analysis*, SAE Technical Paper 2004-01-0922, 2004, doi:10.4271/2004-01-0922.

[16] Pipitone, E., Beccari, A., and Beccari, S., *The Experimental Validation of a New Thermodynamic Method for TDC Determination*, SAE Technical Paper 2007-24-0052, 2007, doi:10.4271/2007-24-0052.

[17] Tazerout, M., Le Corre, O., and Rousseau, S., *TDC Determination in IC Engines Based on the Thermodynamic Analysis of the Temperature-Entropy Diagram*, SAE Technical Paper 1999-01-1489, 1999, doi:10.4271/1999-01-1489..

[18] Nilsson, Y. and Eriksson, L., *Determining TDC Position Using Symmetry and Other Methods*, SAE Technical Paper 2004-01-1458, 2004, doi:10.4271/2004-01-1458.

[19] Chang H, Zhang Y, Chen L., An applied thermodynamic method for correction of TDC in the indicator diagram and its experimental confirmation, Appl Therm Eng. 2005;25(5-6):759-68.

[20] Marek, J.S., *Thermodynamic determination of T.D.C. in piston combustion engines*, in *SAE International Congress and Exposition*1996, SAE International Warrendale Pennsylvania USA: Detroit, Michigan, SAE Paper Number 960610

[21] Finol, C.F., *Heat transfer investigations in a modern Diesel engine*, PhD Thesis, 2008, Dept. of Mechanical Engineering, University of Bath, Bath

[22] Randolph, A.L., Methods of processing cylinder-pressure transducer signals to maximize data accuracy, SAE Paper Number 900170, 1990

[23] Lee, K., Kwon, M., Sunwoo, M., and Yoon, M., *An In-Cylinder Pressure Referencing Method Based on a Variable Polytropic Coefficient*, SAE Technical Paper 2007-01-3535, 2007, doi:10.4271/2007-01-3535.

[24] Miles, P., *The Influence of Swirl on HSDI Diesel Combustion at Moderate Speed and Load*, SAE Technical Paper 2000-01-1829, 2000, doi:10.4271/2000-01-1829.

[25] Payri F, Lujan JM, Martin J, Abbad A., Digital signal processing of in-cylinder pressure for combustion diagnosis of internal combustion engines, Mechanical Systems and Signal Processing. 2010;24(6):1767-84.

[26] Rohrer, R. and Chehroudi, B., *Preliminary Heat Release Analysis in a Single-Cylinder Two-Stroke Production Engine*, SAE Technical Paper 930431, 1993, doi:10.4271/930431.

[27] Zhong, L., Henein, N.A., and Bryzik, W., Effect of smoothing the pressure trace on the interpretation of experimental data for combustion in diesel engines, in SAE 2004 World Congress and Exhibition2004, SAE International Warrendale Pennsylvania USA: Detroit, Michigan. SAE Paper Number 2004-01-0931

[28] Mladek M, Onder CH., A Model for the Estimation of Inducted Air Mass and the Residual Gas Fraction using Cylinder Pressure Measurements, SAE Paper No. 2000-01-0958. 2000.

[29] Colin G, Giansetti P, Chamaillard Y, Heigelin P., *In-Cylinder Mass Estimation using Cylinder Pressure*, SAE Paper No. 2007-24-0049. 2007.

[30] Worm, J., An Evaluation of Several Methods for Calculating Transient Trapped Air Mass with Emphasis on the “Delta P” Approach, SAE Technical Paper 2005-01-0990, 2005,

[31] Lapuerta M, Armas O, Hernandez JJ., Diagnosis of DI Diesel combustion from in-cylinder pressure signal by estimation of mean thermodynamic properties of the gas, Appl Therm Eng. 1999;19(5):513-29, DOI: 10.1016/S1359-4311(98)00075-1

[32] Eriksson, L., Requirements for and a Systematic Method for Identifying Heat-Release Model Parameters, SAE Technical Paper 980626, 1998, doi:10.4271/980626.

[33] Schulze T, Wiedemeier M, Schuette H., *Crank Angle - Based Diesel Engine Modeling for Hardware-in-the-Loop Applications with In-Cylinder Pressure Sensors*, SAE International; 2007., DOI: 10.4271/2007-01-1303, SAE Paper Number 2007-01-1303

[34] Ladommatos, N., Abdelhalim, S.M., Zhao, H. and Hu, Z., The dilution, chemical, and thermal effects of exhaust gas recirculation on diesel engine emissions~Part 1: Effect of reducing inlet charge oxygen, in SAE International Spring Fuels and Lubricants Meeting and Exposition1996, SAE International Warrendale Pennsylvania USA: Dearborn, Michigan. SAE Paper Number 961165

[35] Ladommatos, N., Abdelhalim, S.M., Zhao, H. and Hu, Z., *Effects of EGR on heat release in diesel combustion*, in *SAE International Congress and Exposition*1998, SAE International Warrendale Pennsylvania USA: Detroit, Michigan. SAE Paper Number 980184

Table 1: Compilation of published data comparing the sensitivity of output parameters from heat release analysis to a given uncertainty in input parameters (data is obtained from fired engine simulation [5], fired engine test [6], and motored test [7])

Inputs Parameter		Variation	Data source	Max Output Error IMEP	HR_{max}	Q_c	SOC	Q_w
1	Correct Phasing of cylinder volume (TDC position)	±1°	Motored engine test		2.6%	1.6%		
		±0.5°	Fired engine simulation	3.6%	2.5%		0.8°	<1%
		±1°	Fired engine test	3%				
2	Reference pressure	±0.3bar	Motored engine test		2.5%	0.4%		
		±0.2bar	Fired engine simulation	<1%	<1%		1.2°	2.4%
3	Transducer calibration	±10%	Motored engine test		2.0%	0.2%		
		±4%	Fired engine test	4%				
4	10kHz Low pass filter	N/A	Fired engine test	2%				
5	Trapped mass (m_{cy})	±10%	Motored engine test		0.8%	<0.1%		
		±6%	Fired engine simulation	<1%	1.7%		0.3°	7.4%
6	Compression ratio	±1	Motored engine test		2.5%	0.9%		
		±0.75	Fired engine simulation	<1%	<1%		1.2°	2.4%
7	Convective Heat transfer coefficient	±70%	Motored engine test		2.5%	0.5%		
		±87.7%	Fired engine simulation	<1%	4.3%		1.1°	38.8%
8	Blow-by ($\dot{m}_{bb}$)	±10%	Fired engine simulation	<1%	<1%		<0.1°	<1%

Table 2: Summary of key instrumentation sensors

Low frequency Channel	CP Engineering Cadet Automation system Sensor
Fuel Flow	CP FMS1000 Gravimetric Flow Meter
Air Flow	ABB Sensy flow hot wire flow meter
Gas Pressure	Piezo-resistive pressure transducers
Gas Temperature	k-type thermocouple 1.5mm
Engine Torque	HBM analogue torque sensor

High Frequency Channel	D2T Osiris System Sensor
In-cylinder pressure	Kistler Piezoelectric Pressure Sensor (Type 601) installed in glow plug adaptor
Fuel rail pressure	Kistler Piezoelectric Pressure sensor (Type 601) installed on rail supply pipe.
Injector current	Picotech current clamp

Table 3: Parameter variation and sensitivity results from the test data; results which were below 1% or 0.1° have been omitted for clarity (Mid operating point: 2500rpm / 120Nm)

Inputs				**Output Error**				
Parameter			**Variation**	**IMEP**	**HR_{max}**	**Q_c**	**SOC**	**Q_{HT}**
1	TDC position	2 Std	±0.5°	3.1%	2.8%	2.8%	2.1°	0.6%
		Mean		4.8%	4.2%	3.9%	0.92°	1.8%
		Mid-point		4.6%	3.4%	3.7%	1.2°	1.8%
2	Reference pressure	2 Std	±0.2bar		0.2%	4.8%	0.14°	2%
		Mean				3.9%		1.3%
		Mid-point				3.4%		
3	Transducer calibration	2 Std	±10%		0.6%	0.5%	0.16°	4.1%
		Mean		10%	12%	11%		20%
		Mid-point		10%	12%	11%		20%
4	Trapped mass (m_{cy})	2 Std	±6%		0.37%	0.29%	0.11°	1.4%
		Mean			1.3%			5.9%
		Mid-point			1.1%			5.9%
5	Compression ratio	2 Std	±0.75		4.7%	0.3%	0.91°	0.96%
		Mean			2.3%		0.41°	2%
		Mid-point						2%
6	Heat transfer coefficient	2 Std	±87.7%		3.6%		0.85°	1.4%
		Mean			5.2%		0.41°	85%
		Mid-point			4.8%		0.45°	85%
7	Ratio of specific heats (γ)	2 Std	±0.3		8.3%	1.7%	0.81°	35%
		Mean			9.1%	1.5%	0.38°	23%
		Mid-point			9.3%	1.5%	0.3°	23%

Table 4: TDC fit & error

Model	**R^2**	**Mean error (°*CA*)**	**Max error (°*CA*)**	**2 SD (°*CA*)**
Loss Function Method [16]	0.36	0.076	0.25	0.20
Inflection Point Method [20]	0.53	-0.019	0.26	0.30
Filling and Emptying Model Method	0.85	0.031	0.096	0.071

Table 5: Pegging method results

Model	SSE	R^2	Mean error (bar)	Max error (bar)	2 SD (bar)
Intake manifold	0.0992	0.998	0.032	0.12	0.053
Fixed polytropic constant	0.0856	0.996	-8.5×10^{-3}	0.11	0.076
Variable polytropic constant	6.267	0.831	0.16	1.5	0.58

Table 6: Trapped mass prediction results

Model	SSE	R^2	Mean error (%)	Max abs. error (%)	2 SD of error (%)
Perfect gas law	1.64×10^{-7}	0.999	5.0	6.7	4.1
Perfect gas law (corrected)	2.82×10^{-9}	0.999	-1.4	1.9	1.9
delta-p method	1.90×10^{-9}	0.990	-0.64	2.6	3.4

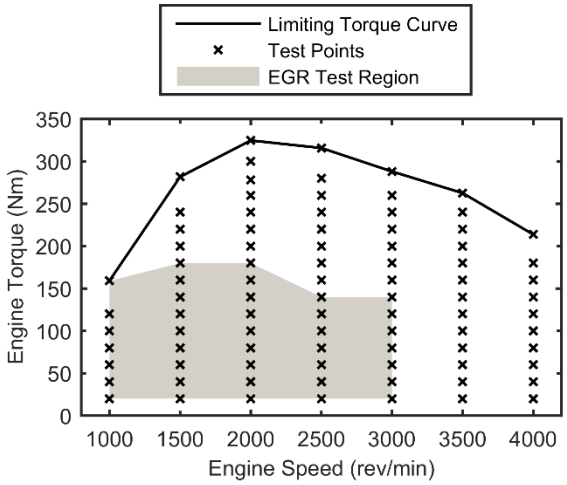

Figure 1: Location of test points for data capture

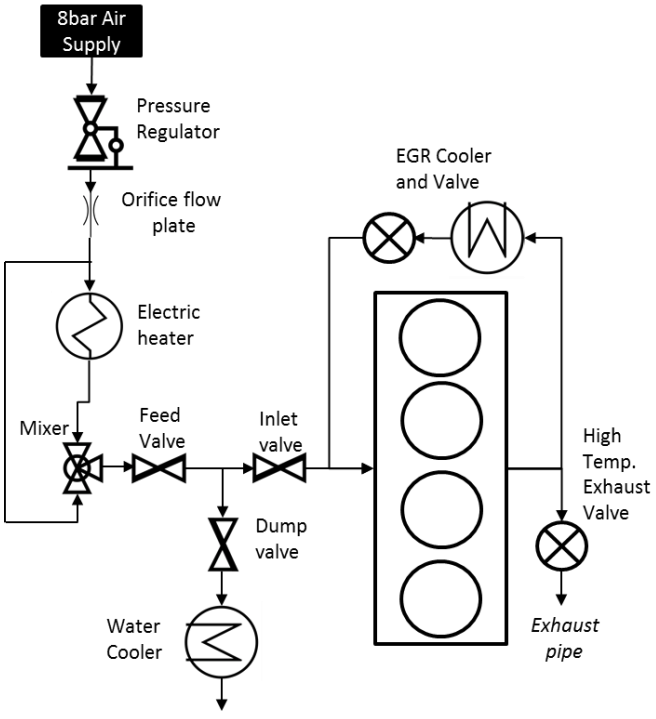

Figure 2: Engine air path configuration with turbocharger emulation hardware

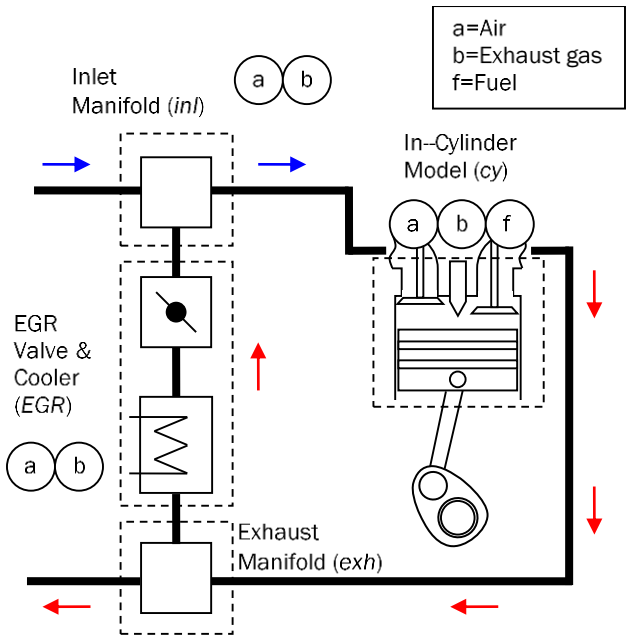

Figure 3: Layout of the filling and emptying model

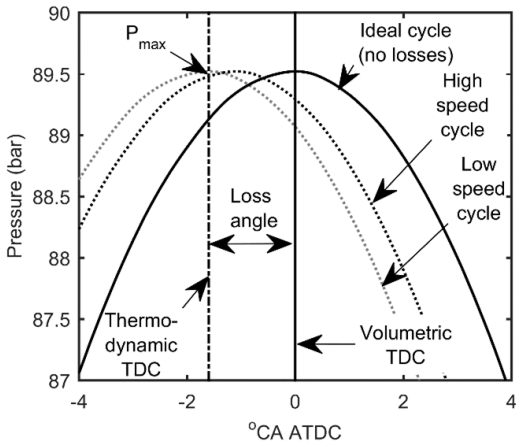

Figure 4: Motored pressure illustrating thermodynamic and volumetric TDC and loss angle

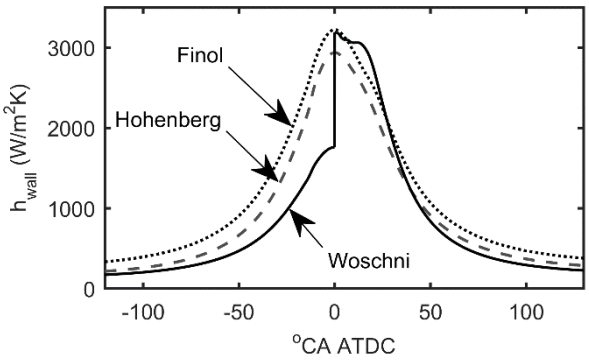

Figure 5: Heat transfer coefficients as calculated by the three different correlations at2500rpm, 120Nm

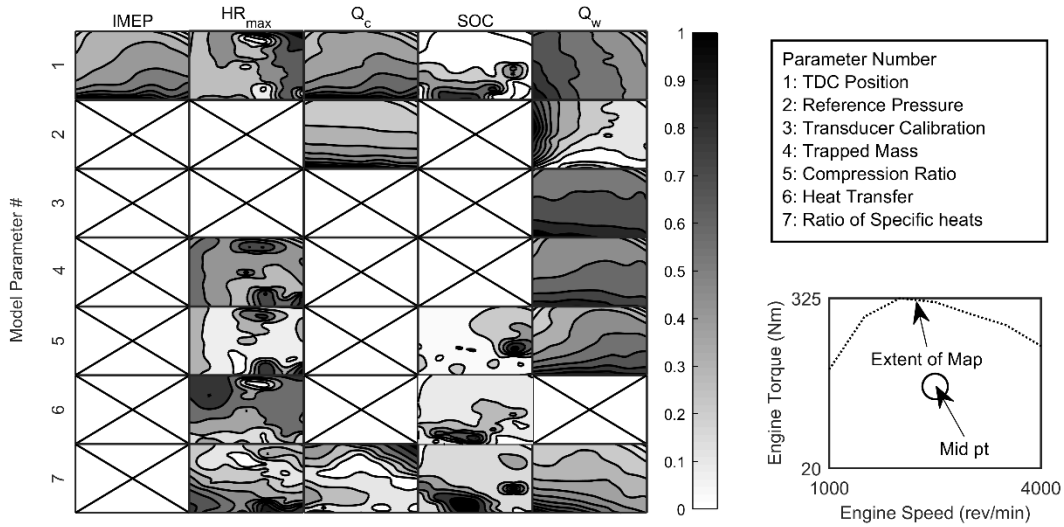

Figure 6: Parameter variation over different speed and load test points, normalised by dividing by the maximum variation (parameters with little variation have been omitted for clarity)

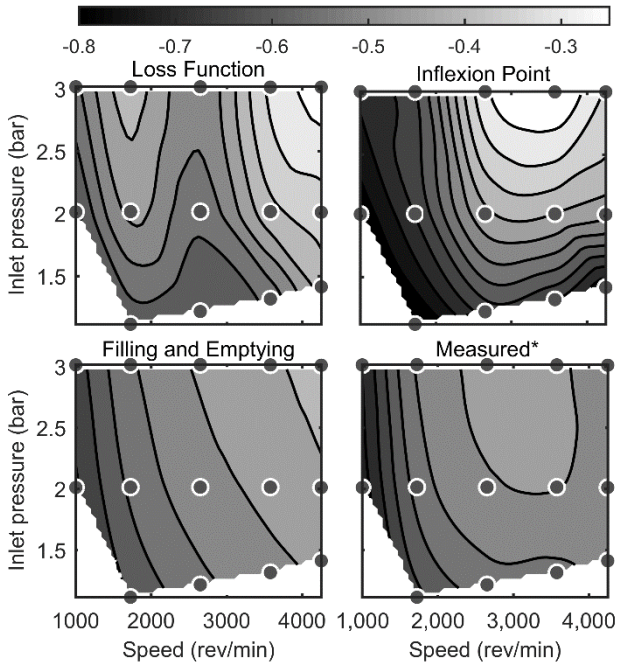

Figure 7: Predicted α_{TDC} compared with measured α_{TDC} for different inlet pressure and speed points using an interpolating cubic spline surface fit (contour) to the data point (circles)

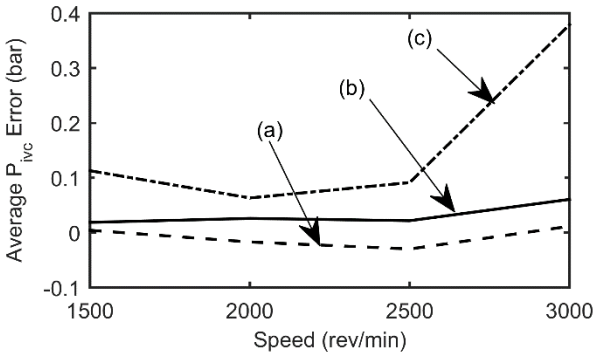

Figure 8: Mean pegging error compared to the filling and emptying model against speed for (a) fixed polytropic constant pegging, (b) intake manifold pressure pegging, and (c) variable polytropic constant pegging

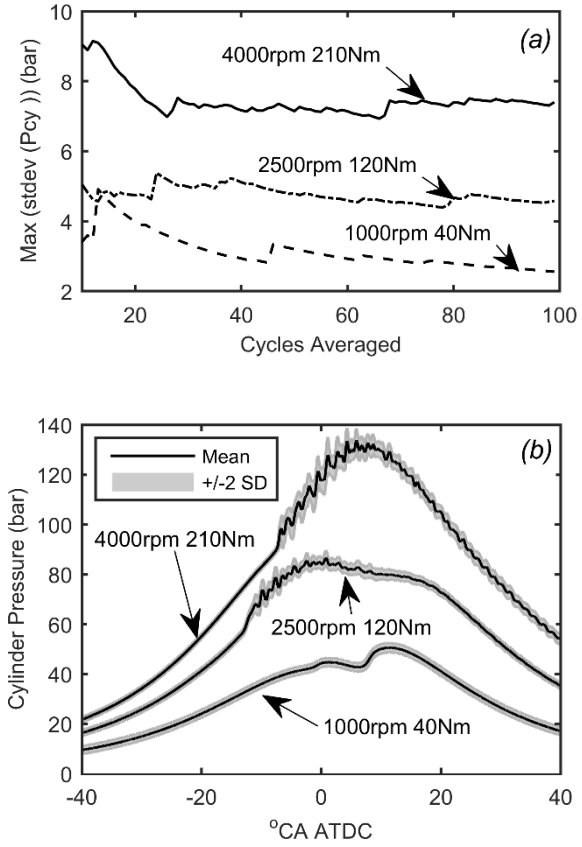

Figure 9: Cyclic variability at different operating conditions - (a) maximum standard deviation vs cycles averaged, (b) standard deviation and mean signal at different points

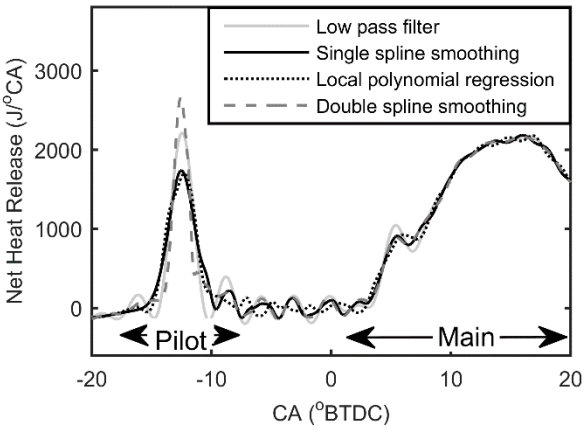

Figure 10: Comparison of different filter techniques at 2500rpm, 120Nm

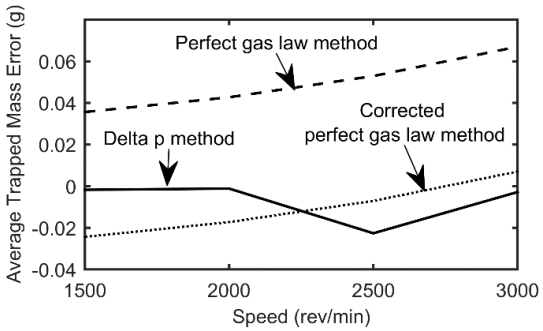

Figure 11: Average trapped mass prediction error vs. engine speed

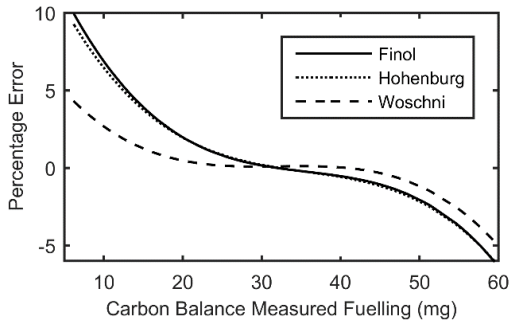

Figure 12: Average percentage error in estimated fuel burnt vs. measured fuel consumption with different heat transfer models

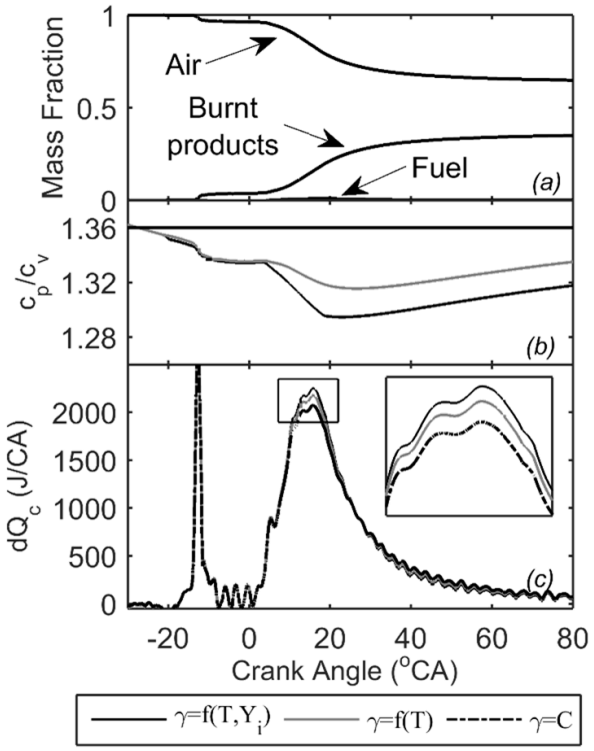

Figure 13: For the operating condition 2500rpm, 120Nm, (a) Gas fraction model output, (b) Ratio of specific heats and (c) Gross RoHR illustrating the impact of three different assumptions for ratio of specific heats: 1. function of gas composition and temperature, 2. Function of temperature only, 3. A constant value

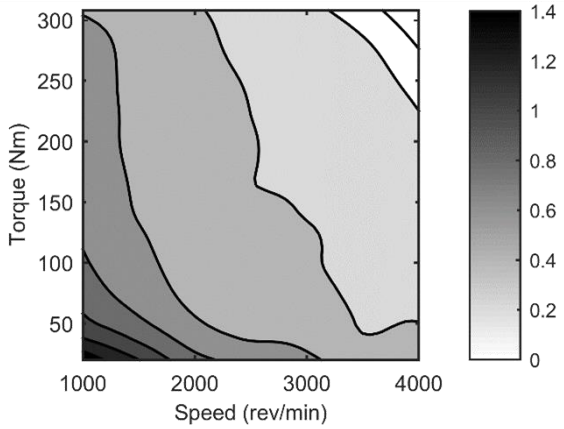

Figure 14: Percentage contribution to gross heat release from blow-by losses